High-power, near-diffraction-limited, narrowband ring optical parametric oscillator with counterdirectional mode coupling at 1.53 μm

IOP Publishing | Astro Ltd Laser Physics

Laser Phys. **28** (2018) 095404 (6pp) https://doi.org/10.1088/1555-6611/aacc15

High-power, near-diffraction-limited, narrowband ring optical parametric oscillator with counterdirectional mode coupling at 1.53 μm

X H Zheng[1], **B F Zhang**[1], **J Guo**[2], **Z X Jiao**[1] **and B Wang**[1,2]

[1] School of Physics, Sun Yat-sen University, Guangzhou 510275, People's Republic of China
[2] Sino-French Institute of Nuclear Engineering and Technology, Sun Yat-sen University, Guangzhou 510275, People's Republic of China

E-mail: jiaozhx@mail.sysu.edu.cn and wangbiao@mail.sysu.edu.cn

Received 28 September 2017, revised 11 June 2018
Accepted for publication 11 June 2018
Published 17 July 2018

Abstract

A continuous-wave (CW) singly resonant optical parametric oscillator (OPO) employing a volume Bragg grating (VBG) in a ring resonator is demonstrated. Similar to a linear cavity, the minute absorption induces surface distortion and frequency shift in both nonlinear crystal and grating. The joint thermal effects are proved to account for the unconventional OPO performance in regard to power stability, spectrum and beam quality. However, counterdirectional mode coupling of the signal at ~1.53 μm with considerable power is first observed from the VBG-based resonator and what theory suggests would be a unidirectional ring. This is believed to originate from the grating structure and has some influence on threshold and stability of the OPO. Up to 4.6 W of narrowband (~0.09 nm), diffraction limited ($M^2 \leqslant 1.2$) radiation at 1.53 μm has been obtained in our experiment, together with 2.8 W of output idler at 3.49 μm.

Keywords: volume Bragg grating, singly resonant OPO, ring cavity, counterdirectional mode coupling

(Some figures may appear in colour only in the online journal)

1. Introduction

Continuous-wave (CW) optical parametric oscillators (OPOs) providing high-power, narrow-linewidth radiation from near- to mid-infrared are outstanding candidates required for applications in high-resolution molecular spectroscopy [1, 2], trace gas detection [3, 4], atom physics [5], and quantum optics [6]. Moreover, with narrow-linewidth even single-frequency radiation at telecom band, particularly with wavelength at 1.5–1.6 μm, CW OPOs are also unique sources for realizing entanglement-based quantum key distribution system on optical fiber networks. This permits long-distance communication over standard single-mode fiber since the transmit losses at these telecommunication wavelengths are minimized [7–9].

Apart from CW OPOs, several approaches have also been developed to obtain narrow-linewidth 1.5–1.6 μm radiations, for example, erbium fiber lasers and diode-pumped Er, Yb-codoped solid-state lasers [10, 11]. However, a CW singly resonant OPO based on a volume Bragg grating (VBG-OPO) shows great advantages in high output power, wide tunable range, spectral narrowing and stabilization, due to the narrow diffraction bandwidth, high peak reflectivity and sensitive angular selectivity of VBG [12–14]. The VBG acts simultaneously as an output coupler and spectral filter, making the OPO system compact and simple to fulfill the requirements of applications. As for the resonator type, a ring resonator is supposed to greatly suppress back conversion compared with a linear resonator because it is operating unidirectionally and hence with negligible feedback of parametric beams. Moreover, thermal

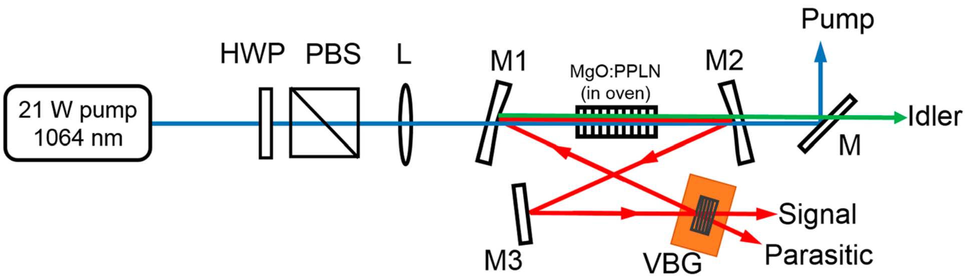

Figure 1. Schematic of the CW VBG-OPO based on a four-mirror bow-tie ring cavity.

effects induced by absorption of the intensive signal power are reduced since the signal beam only passes the crystal once per roundtrip. Therefore, a ring configuration is considered to have superior power stability and spectral performance to a linear one when achieving high-power 1.5–1.6 μm radiation.

In this letter, we demonstrate a singly resonant OPO based on a periodically poled lithium niobate (PPLN) crystal, and a VBG is used as a reflective element of the four-mirror bow-tie ring cavity. With up to 21 W of CW pump power at 1064 nm, narrowband 1.53 μm radiation has been achieved. Performances of the configuration with regard to output power, stability, spectrum and beam quality are investigated. Similar to our previous works of another VBG-OPO with a linear cavity [15], the spectral narrowing effect of the VBG is confirmed by comparing with another OPO employing a common partially reflective mirror as output coupler (OC-OPO), while the power and beam quality performances at different operation point are interpreted by the joint thermal effects of the VBG and PPLN. Moreover, counterdirectional mode coupling has been observed from the theoretically unidirectional ring resonator, which is first reported here in a VBG-based OPO, and is believed to be originated from the grating structure of the quasi-phase-matching (QPM) crystal [16].

2. Experimental setup

A schematic of our experimental setup is depicted in figure 1. The pump system consists of a commercial CW Nd:YVO_4 solid-state laser and a two-stage amplifier, delivering up to 21 W output power at 1064 nm with a TEM_{00} spatial mode (M_x^2 ~ 1.2, M_y^2 ~ 1.1). Power stability of the pump system is measured to be 0.27% rms within 60 min. To maintain stable output characteristics, the pump system is operating at maximum power. A combination of a half-wave plate (HWP) and a polarizing beam splitter (PBS) is used as variable attenuator in order to change the input pump power for OPO without disturbing the pump system. The pump beam is tightly focused to yield a beam waist radius of ~40 μm inside the PPLN crystal by a singlet lens ($f = 75$ mm), corresponding to a focusing parameter of ξ_p ~ 2.5 [17]. The OPO cavity is a standard four-mirror bow-tie ring that comprises three mirrors and a reflective VBG. The mirrors in cavity are highly reflective ($R > 99.9\%$) for the signal and transparent for the idler and pump to ensure single resonance. The geometric separation between the concave mirrors M1 and M2 ($r = 100$ mm) is 140 mm, and the total length of the OPO cavity is 0.64 m. The resonant signal in the cavity has a beam radius of ~55 μm at the center of the crystal, corresponding to a focusing parameters of ξ_s ~ 1.9, slightly deviating from ξ_p.

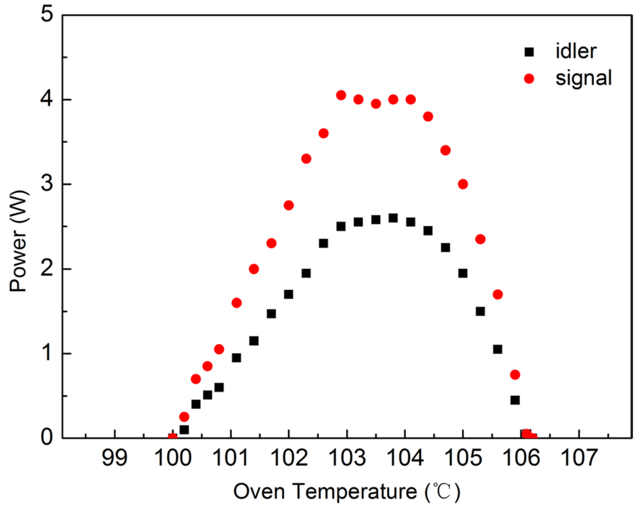

Figure 2. Outpupt power versus oven temperature at a pump power of 21 W.

A 50 mm-long MgO:PPLN (HC Photonics Corp.) is used as nonlinear crystal; both end faces are antireflection-coated with 0.2, 0.5, and <5% reflectance at the pump, signal and idler wavelengths, respectively. One of the crystal faces is angle-polished (0.7°) to avoid residual etalons. In our experiment, the crystal is operating in a poling period of 30.0 μm for a phase matching at the VBG reflection peak. The crystal is housed in an oven of which the temperature can be stabilized within ±0.1 °C ranged from room temperature to 200 °C. A small folding angle around 5° is chosen to minimize astigmatism. In this case, the peak reflectivity of the VBG (Ondax 114-er217-001) is specified as ~97% at wavelength around 1529 nm with a bandwidth of ~0.8 nm. The VBG substrate, in a dimension of $2 \times 2 \times 2\,\text{mm}^3$, is covered with indium foil and mounted in a copper carrier. The copper carrier is a circular plate in diameter of 25.4 mm and in thickness of 7 mm and served as a heat sink without any active temperature stabilization. With antireflection coating, the reflectivity of the VBG substrate is specified as <0.5% per surface at signal wavelength. A dichroic mirror M separates the generated idler output from the residual pump and signal radiation.

3. Results and discussions

To find the optimal operating point of the VBG-OPO at 20 W of pump power, temperature of the PPLN was tuned around

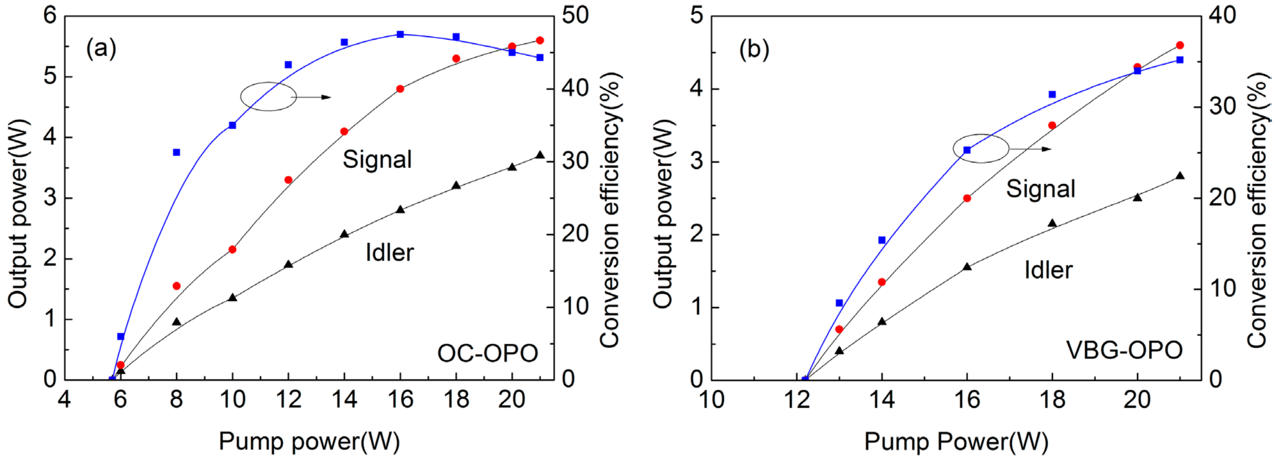

Figure 3. Measured output power versus pump power in (a) OC-OPO and (b) VBG-OPO. Oven temperatures are 103.5 °C in both configurations. The solid curves are guide to the eye.

the theoretical matching value. The output signal and idler power are showed in figure 2. The temperature tuning curves are clearly asymmetric and similar to those we have obtained in a linear cavity [15]. As previously reported, a minute absorption of the intracavity power results in a temperature rising of PPLN, and hence a frequency shift of phase-matching wavelength λ_p for the parametric process, or a redshift of peak reflectivity λ_v of VBG [18, 19]. In our previous experiment, the shift rate of λ_p around 1.53 μm versus intracavity power has been calculated to be −0.37 GHz/W, while for λ_v, it is 0.21 GHz/W. It should be noted that in a linear cavity, the power value on VBG is the same as the intracavity power. However, in a ring cavity where VBG is served as an output coupler, this value can be almost twice of the intracavity power. This implies that the shift rate of λ_v versus intracavity power in ring cavity should be around 0.42 GHz W^{-1}, which is twice of that in a linear cavity. Therefore, the thermal wavelength shift of VBG is greater than that of PPLN in our ring resonator, which explains the asymmetry of temperature tuning curves in figure 2 [15]. Giving an output signal power of 4.6 W at 21 W of pump power and frequency scan rate of 1.6 GHz K^{-1} [12], the according temperature rise of the VBG is calculated to be 40 °C, in good agreement with the result of 43 °C from a thermal imager. The plateau around 103.5 °C implies a small decrement of peak reflection of the VBG under high flux irradiation [19].

We measured the output power as a function of pump power in a VBG-OPO and an OC-OPO, where the output coupling efficiency is 3% and 1.5%, respectively. The oven temperature is 103.5 °C in both configurations. As presented in figure 3, the maximum power of idler and signal from the OC-OPO is 3.7 W and 5.6 W, respectively. The total maximum conversion efficiency of 47.5% is achieved at a pump around 2.8 times of the threshold, which is close to the theoretical value of $(\pi/2)^2$ in the plane-wave approximation. For the VBG-OPO, 2.8 W of idler power and 4.6 W of signal power are obtained at 21 W of pump power. Due to the relatively high threshold, we are not able to pump at more than 2 times above the threshold. Thus the conversion efficiency keeps increasing with pump power to a maximum value of 35.2%. In addition, we obtain considerable parasitic output coupling in counter direction from both

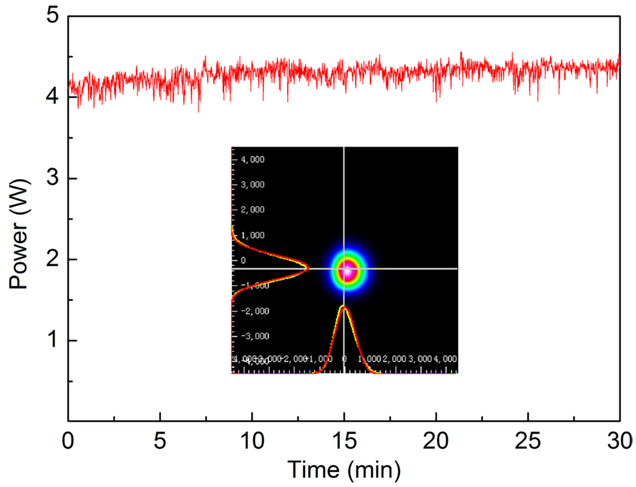

Figure 4. Idler power stability of the VBG-OPO. Insert is beam profile of signal with a power of 4.6 W.

OPOs which are supposed to be unidirectional rings. This has also been observed in a ring OPO based on orientation-patterned gallium arsenide [20]. A detailed investigation by simulation as well as experiment attributed the counterdirectional output coupling to the fluctuations of the QPM grating structure parameters, such as period length or refraction index of every small domain in QPM gratings [16]. In our experiments, the counterdirectional power are believed to originate from both the imperfect antireflection coating surfaces and the Bragg structure of the PPLN crystal. By angle-tilting the crystal, the parasitic output power slightly decreases, mainly because the reflective signal beam from the crystal surfaces also rotates off axis and is block by the VBG holder, since the VBG has an aperture of only $2 \times 2\,mm^2$ and is used at an oblique angle. However, the parasitic output coupling cannot be completely eliminated, which suggests that still large part of the backward reflection results from the Bragg structure of the PPLN. In the VBG-OPO, the corresponding parasitic output power are around 0.4 W, 0.8 W and 0.8 W corresponding to output signal power of 1.15 W, 2.5 W and 4.6 W, respectively, showing that the parasitic output power is not proportional to the intracavity power. This, in agree with

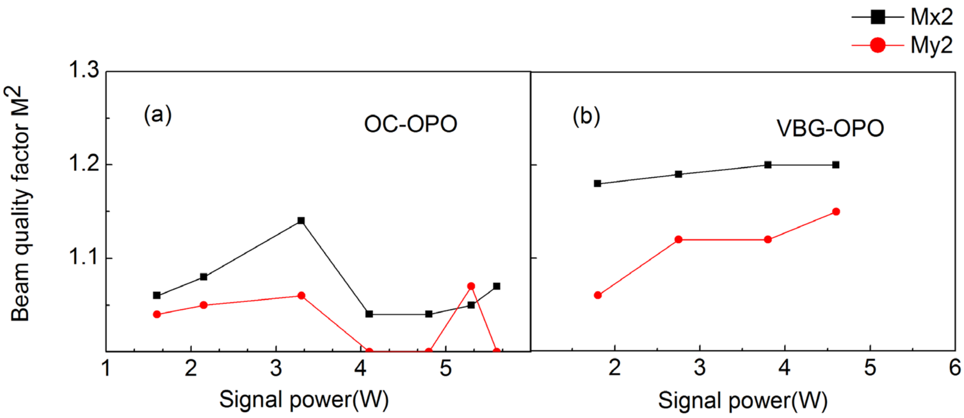

Figure 5. Quality factors of the signal beam versus output signal power in OC-OPO (a) and VBG-OPO (b).

[16], indicates a strong and irregular reflectivity dependence on wavelength considering the thermal wavelength shift of the PPLN, which can result in an increase of operating threshold and instability of the OPO as suggested.

The threshold of a singly resonant OPO in case of confocal Gaussian beams, can be simply given by $P_{th} = \Theta(T_s + V_s)$. It is obvious that the threshold is proportional to the overall cavity loss per roundtrip for the resonant signal $T_s + V_s$, where T_s stands for the output coupling loss and V_s all the other residual losses. The parameter Θ is a constant and can be calculated according to [14]. Given the threshold of 5.7 W and the output coupling loss as 1.5% in OC-OPO, the sum of all residual losses for the signal wavelength inside the cavity is estimated to be 2.7%. Apart from the reflection loss of the PPLN surfaces at signal wavelength, the remaining loss, mainly the backreflection of the Bragg structure and absorption of the crystal, account for almost 1.7% of signal loss inside the cavity. As for the VBG-OPO, threshold of 12.2 W and extraction efficiency of 3% result in the overall parasitic loss of 6%. Among 3.3% increase of loss compared with OC-OPO, about 1% is caused by the antireflection coating of the VBG substrate surface which is transverse twice by the reflected signal, while the other 2.3% should be attributed to absorption and other losses by the VBG.

The signal power exhibits a stability of 2.6% rms within 30 min with ~4.3 W of power, as showed in figure 4. Since the pump system has a much better stability performance, we attribute the strong fluctuation in output power mostly to the joint thermal effects of the PPLN and VBG as interpreted in our last experiment [15], and also the high sensitivity of the ring resonator where optical elements are used at oblique angles. The random air current over the OPO causes pressure and temperature alterations within the cavity and around elements. Without active stabilization, temperatures of heat sink and VBG change. In this way, a consequent reflection peak shift is suggested. Moreover, by shacking the mirrors, inducing gradients in the air refractive indexes, the cavity length and optical paths of the ring cavity can easily change. Last but not least, the parasitic output coupling in counter direction also have a strong effect on frequency and power stabilities. All these effects are responsible for the power fluctuation. Realignment is needed to restart the OPO once the operating system is blocked for several seconds, confirming the strong thermal induced frequency shift and optical paths change.

The output beams seem to be almost diffraction limited and of very high beam qualities. M^2 values are measured to be $\leqslant$1.2 in both configurations by a laser beam analyzer (Thorlab, BP209-VIS/M). An example of the output signal beam profile from the VBG-OPO in TEM_{00} mode ($M_x^2 = 1.2$, $M_y^2 = 1.15$) is showed as insert in figure 4, with 4.6 W output power. Other results are shown in figure 5. Beam qualities are generally worse in VBG-OPO than those in OC-OPO due to thermal distortion of the VBG. It is notable that the beam qualities of OC-OPO improve when signal output power is higher than 4.1 W, corresponding to an actual intracavity power of more than 320 W if we take 0.8 W of parasitic output coupling in another direction into consideration. This is probably owing to a thermal waveguide that increase the mode overlap and hence improve the beam quality [20, 21]. While in VBG-OPO, apart from the thermal distortion effect, the VBG can also act as a spatial filer. As has been pointed out in [22], VBG can show transverse mode selectivity when used at an oblique incidence angle with a finite beam size. The beam quality in x-direction is generally inferior to that in y-direction even after rotating the VBG by 90°, which is believed to be related with the pump beam quality and the thermal dissipation of the PPLN.

The spectra around 1.53 μm are measured with a monochromator (iHR550, HORIBA), and all the results are average traces of 5 sweeps, as depicted in figure 6. In the OC-OPO, the spectrum is evidently broad and unstable with 3.4 W of output signal power (figure 6(a)), due to the multi-longitudinal mode pump laser and sufficient parametric gain. The corresponding parasitic signal shows a similar spectrum, with the power up to 1.4 W (figure 6(b)). As for the VBG-OPO, the spectra are substantially narrower (~0.09 nm) and more stable compared with that in OC-OPO. The spectrum of parasitic output with 0.4 W of power is identical with that of the signal at 1.15 W (figures 6(c) and (d)), implying that the parasitic output mostly occurs through the counterdirectional coupling of the PPLN grating structure, rather than other nonlinear process. Note that the signal wavelength changes with output power (figures 6(c), (e) and (f)), confirming the thermal induced wavelength shift in VBG and PPLN.

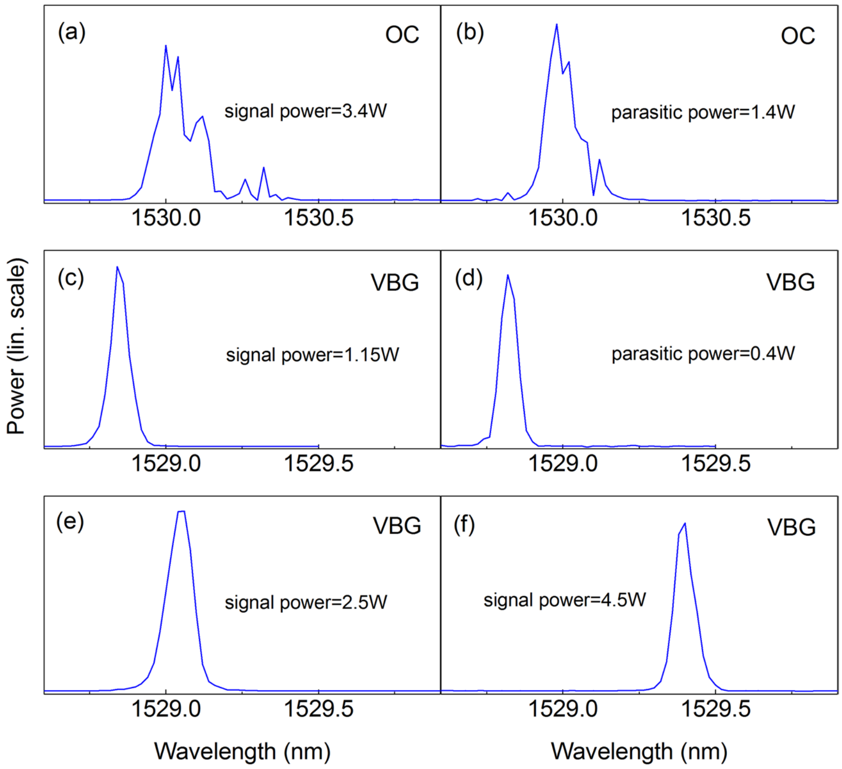

Figure 6. Spectra of signal and parasitic output coupling beam in (a) and (b) OC-OPO and (c)–(f) VBG-OPO.

4. Conclusion

For CW OPOs employing PPLN as nonlinear crystal and VBG as a cavity element, minute absorption of intensive intracavity power can result in strong thermal effects. The asymmetric temperature tuning curves of power, beam qualities and spectra are well interpreted by the joint thermal effects of the PPLN and VBG, which has also been reported in our previous experiments of linear cavity VBG-OPOs. However, the unexpected parasitic output coupling signal in counterdirection has been observed in our OPOs with ring cavities. This parasitic mode coupling, which strongly and irregularly depends on wavelength and the QPM grating period, give birth to an increase of threshold and instability of the OPO. On the other hand, it provides us extra radiation output at 1.53 μm and has an identical spectrum with the primary signal. Finally, up to 5.4 W (4.6 W of primary and 0.8 W of parasitic) of narrowband 1.53 μm radiation with diffraction limited profile has been obtained from our OPO, which is of great interest in many applications.

Acknowledgments

This work was supported in part by the National Natural Science Foundation of China under Grant 61308056 and 11204044, and the PhD Start-up Fund of Natural Science Foundation of Guangdong Province under Grant 61308056.

References

[1] Kovalchuk E V *et al* 2001 High-resolution Doppler-free molecular spectroscopy with a continuous-wave optical parametric oscillator *Opt. Lett.* **26** 1430–2

[2] Zaske S, Lee D H and Becher C 2010 Green-pumped cw singly resonant optical parametric oscillator based on MgO: PPLN with frequency stabilization to an atomic resonance *Appl. Phys.* B **98** 729–35

[3] Van Herpen M *et al* 2006 Optical parametric oscillator-based photoacoustic detection of CO_2 at 4.23 μm allows real-time monitoring of the respiration of small insects *Appl. Phys.* B **82** 665–9

[4] Cristescu S M *et al* 2008 Laser-based systems for trace gas detection in life sciences *Appl. Phys.* B **92** 343–9

[5] Mickelson P G *et al* 2009 Repumping and spectroscopy of laser-cooled Sr atoms using the (5s5p)^{3}P2–(5s4d)^{3}D2 transition *J. Phys. B: At. Mol. Opt. Phys.* **42** 235001

[6] Strößner U *et al* 2002 Single-frequency continuous-wave optical parametric oscillator system with an ultrawide tuning range of 550–2830 nm *J. Opt. Soc. Am.* B **19** 1419–24

[7] Takesue H and Inoue K 2005 Generation of 1.5 μm band time-bin entanglement using spontaneous fiber four-wave mixing and planar light-wave circuit interferometers *Phys. Rev.* A **72** 041804

[8] Honjo T *et al* 2008 Long-distance entanglement-based quantum key distribution over optical fiber *Opt. Express* **16** 19118–26

[9] Li Y *et al* 2015 CW-pumped telecom band polarization entangled photon pair generation in a Sagnac interferometer *Opt. Express* **23** 28792–800

[10] Feng J *et al* 2008 Noise suppression, linewidth narrowing of a master oscillator power amplifier at 1.56 μm and the second harmonic generation output at 780 nm *Opt. Express* **16** 11871–7

[11] Li Y *et al* 2013 400 mW low noise continuous-wave single-frequency Er, Yb: $YAl_3(BO_3)_4$ laser at 1.55 μm *Opt. Express* **21** 6082–90

[12] Vainio M *et al* 2010 Continuous-wave optical parametric oscillator based on a Bragg grating *Opt. Lett.* **35** 1527–9

[13] Vainio M *et al* 2011 Tuning and stability of a singly resonant continuous-wave optical parametric oscillator close to degeneracy *Opt. Express* **19** 22515–27

[14] Zeil P *et al* 2014 High-power, single-frequency, continuous-wave optical parametric oscillator employing a variable reflectivity volume Bragg grating *Opt. Express* **22** 29907–13
[15] Zheng X *et al* 2016 Joint thermal effects of VBG and nonlinear crystal in a singly resonant OPO *IEEE Photonics Technol. Lett.* **28** 1107–10
[16] Vasilyev S *et al* 2010 Counterdirectional mode coupling in ring resonators with QPM nonlinear crystals and effects on the characteristics of cw optical parametric oscillation *Appl. Phys.* B **100** 737–47
[17] Guha S, Wu F J and Falk J 1982 The effects of focusing on parametric oscillation *IEEE J. Quantum Electron.* **18** 907–12
[18] Waritanant T and Chung T 2011 Influence of minute self-absorption of a volume Bragg grating used as a laser mirror *IEEE J. Quantum Electron.* **47** 390–7
[19] Tjörnhammar S *et al* 2013 Thermal limitations of volume Bragg gratings used in lasers for spectral control *J. Opt. Soc. Am.* B **30** 1402–9
[20] Lin S T *et al* 2008 Observation of thermal-induced optical guiding and bistability in a mid-IR continuous-wave, singly resonant optical parametric oscillator *Opt. Lett.* **33** 2338–40
[21] Lin S T *et al* 2010 Thermal waveguide OPO *Opt. Express* **18** 1323–9
[22] Hellstrom J E *et al* 2008 Finite beams in reflective volume Bragg gratings: theory and experiments *IEEE J. Quantum Electron.* **44** 81–9